

Experimental and Numerical Studies on Fire Whirls

**K. Matsuyama¹, N. Ishikawa², S. Tanaka²,
F. Tanaka¹, Y. Ohmiya², and Y. Hayashi³**

¹*Center for Fire Science and Technology, Tokyo University of Science,
2641, Yamasaki, Noda-shi, Chiba 278-8510, Japan*

²*Dept. of Architecture, Faculty of Science and Technology, Tokyo University of Science,
2641, Yamasaki, Noda-shi, Chiba 278-8510, Japan*

³*Building Research Institute, 1 Tachihara, Tsukuba-shi, Ibaraki 305-0802, Japan*

Abstract

In case that conflagration such as urban fire occurred, there is case which the swirl flow, so-called fire whirls sometimes generates. The generation of fire whirls is a rare but potentially catastrophic form of fires. In order to control of fire whirls, it is important to specify the generating mechanism. In this paper, experimental and numerical studies are reported on whirling flames, which modeled fire whirls. A propane burner was used as a fire source of experiment apparatus. The distribution of temperature and velocity of fire whirl were measured in experiments. Moreover, the prediction of fire whirls phenomenon was carried out by using CFD code. The CFD code, which is the FDS Ver.3.1 developed in NIST, was used for numerical simulation.

1. Introduction

In the large fire like an urban fire, the fire whirls that is the singular phenomenon might be often generated, and big damage be caused. The fire whirls cause a threat for the surrounding because reaction against combustion is strongly promoted, the flame height progresses by the swirl, the fire brands are scattered widely. For example, Great Kanto Earthquake (in Japan, 1923) and Humburg large air raid

(in Germany, 1943) are typical as the damage case with the fire whirls.

Although the phenomenon of fire whirl reported in previous study, the main focus is instance concerning damage [1, 2]. The other hand, the cause of generation and behavior of fire whirls were researched experimentally and theoretically [3-5]. However, the generation mechanism and behavior of the fire whirls depend on various parameters included contingency such as the meteorological condition. Therefore, it is difficult to clarify quantitatively and qualitatively. Moreover,

Corresponding Author- Tel.: +81-4-7124-1501;

Fax: +81-4-7123-9873

E-mail address: kmatsu@rs.noda.tus.ac.jp

what strategy is effective to prevent generation is not referred.

The purpose of this study is to clarify the generation mechanism and behavior of the fire whirls qualitatively and quantitatively. First of all, the reductively scale model experiments were carried out. Moreover, the numerical simulation of fire whirls phenomenon was carried out by using CFD code.

2. Experimental

2.1 Outline of Experiment

In the large-scale fire whirls generated in Great Kanto Earthquake and the large air raid in Humburg, the external force of global of the Coriolis force and the weather, etc. is thought to be one of the important factors to be generated the fire whirls. However, because it was used a reductive scale model apparatus in this study, these external forces were disregarded. The experiments were carried out on the Full-Scale Fire Laboratory at the Building Research Institute (in Japan).

2.2 Experimental Procedure

The swirl flame was compulsorily generated by setting up the screen assumed to be a building in the fire source surroundings as shown in Figure 1. Because it experimented under calm, the swirl of the flame will be generated for the self-induction current to the flame.

A systematic experiment concerning the following four parameters, which are 1) HRR (Heat Release Rate) of fire source, 2) width of the clearance between screens, 3) distance between center of fire source and screen, 4) height of screen, was carried out. And, the clarification of the generation limit and the behavior were tried.

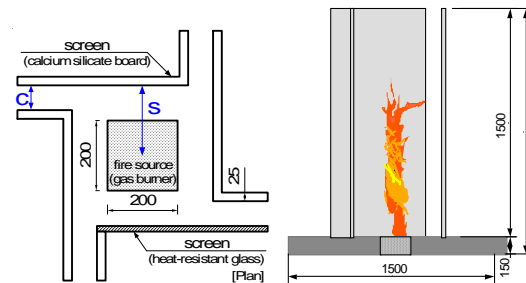


Figure 1. The schematic of experimental model (unit: mm)



Figure 2. The experimental model

2.3 Experimental Model and Measurement Items

(1) Experimental Model

As for the experimental model, the screens of the calcium silicate boards and the heat-resistant glass were set up in surroundings of the gas burner as shown in Figure 1. Distance between the center of fire source and a screen (s) and width of the space between screens (c) are changed by regularly moving the location of the screens. Moreover, height of the screen (h) is changed by regularly moving foundation where the source was put up and down.

The propane gas burner was used for the source. The size of the burner was assumed to be 200 x 200 [mm].

(2) Measurement items and method

The temperature distribution of whirling flames, the height of whirling flames, and flame horizontal flow velocity

were measured. The measurement method of each measurement item is shown in the following. The location of measurement starting point is made to the center of the burner, and made the z axis in the vertical direction, the x axis and the y axis in the horizontal direction of the burner surface.

a) Vertical temperature distribution of whirling flames

To measure vertical temperature distribution of the flame, thermocouple-net installing 48 thermocouples is put in the locations shown in Figure 3. The net has type-K thermocouples (0.65 [mm]-diam.). As shown in Figure 3, vertical temperature distribution was measured.

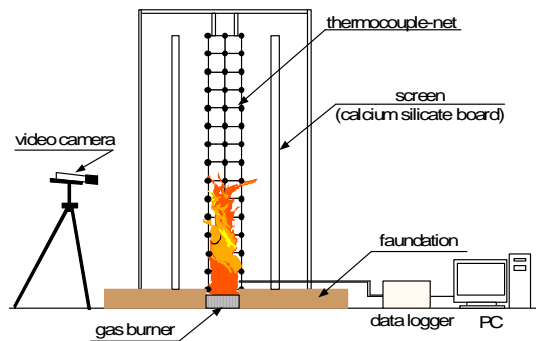


Figure 3. The schematic of the measurement system

b) Height of whirling flame

The height of whirling flames was measured from the district put the heat-resistant glass as one of the screens by using a video camera. Moreover, the swirling duration was analyzed from the video image.

c) Horizontal flow velocity of flame

The horizontal flow velocity of flame was measured by using the PIV (Particle Image Velocimetry) system. The PIV system is a measuring device that can measure the velocity field in the two-dimensional surface from time displacement of the particle imaging to a

simultaneous multipoint. The schematic of the PIV system was shown in Figure 4. The measurement by this system used the following device.

- Camera: MEGAPLUS Camera Model ES 1.0 (KODAK)
- Laser: Pulsed YAG Laser2D (JAPAN LASER Inc.)
- Software: Vid PIV (OXFORD LASERS Co.)

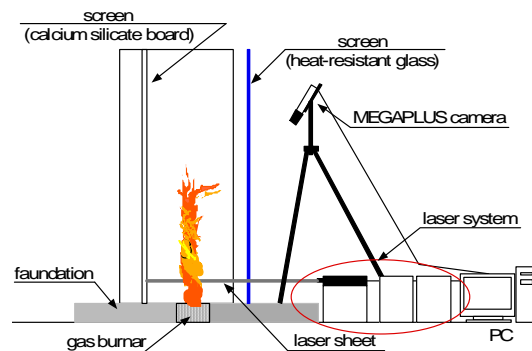


Figure 4. The schematic of the PIV system

2.3 Experimental Condition

Experimental conditions are shown in Table 1. A square gas burner as the fire source is used, a width is 0.2 [m].

Table 1. Experimental conditions

Particulars		Conditions
H.R.R	Q [kW]	10, 15, 20
distance between center of fire source and a screen	s [m]	0.10 - 0.46 (each 0.02)
width of the clearance between screens	c [m]	0.05, 0.10, 0.15
The height of the screen	h [m]	0.5, 1.0, 1.5

As shown Figure 1, the distance between the center of fire source and a

screen (s) was applied to the range of 0.1 to 0.46[m] (each 0.02[m]), the width of the clearance between screens (c) was applied to 0.05, 0.10, and 0.15 [m], the height of the screen (h) was applied to 0.5, 1.0, and 1.5 [m], and HRR of fire source (Q) applied to 10, 15, and 20 [kW].

The heat release rate obtains 10 [kW] from the equation according to similarity law between a reductive scale model and a real large scale as shown in the following [6].

$$\frac{L_f}{L_s} = \left(\frac{Q_f}{Q_s} \right)^{2/5} \quad (1)$$

2.4 Experimental Results

(1) Height of whirling flames

The height of the flame including flame tip was measured for 6 seconds every 0.03 seconds, and the average of the measured value was defined with the height of whirling flames.

The height of whirling flames in case that the width of the clearance between screens (c) was changed was shown in Figure 5, in case that the distance between the center of fire source and a screen (s) was changed was shown in Figure 6, in case of changing the range of height of the screen (h) was changed was shown in Figure 7.

The height of whirling flames was extended as the height of the screen rises as shown in Figure 6. The height of the flame lowers because of close to the free burning when the distance between the center of fire source and a screen expands to some degree. Moreover, the height of the flame lowers because it was located far away flow of the swirl wind, when the distance of between fire source and screens extends, and the width of the clearance narrows. The height of the flame rises because the entrainment air from the upper part of the screens becomes small as the

screen rises, and that has the effect denied the swirl wind from the clearance. That is, the height of whirling flames depends on the ratio of entrainment air from the upper part of the screens and the clearance.

Moreover, the appearance of the fire whirls (comparison between free burning and whirling flames) is shown in Figure 8. It should be noted that the height of whirling flames was stretched extremely compared with free burning.

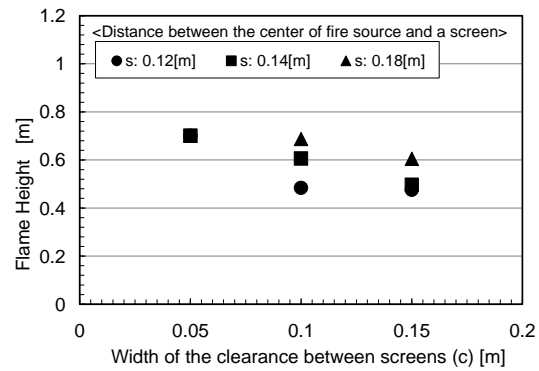


Figure 5. Height of whirling flames in case of changing the range of width of the space between screens (Q :15[kW], h :1.5[m], s :0.12-0.18[m])

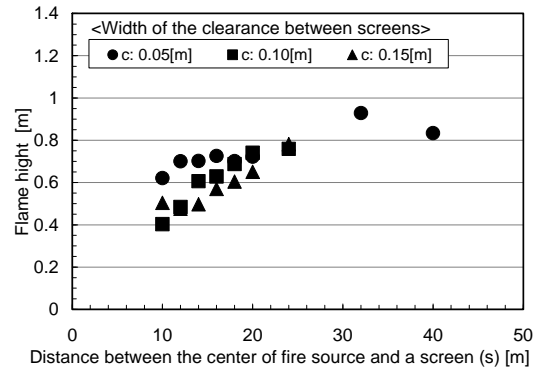


Figure 6. Height of whirling flames in case of changing the range of distance of center of fire source and screen (Q :15[kW], h :1.5[m], c :0.05-0.15[m])

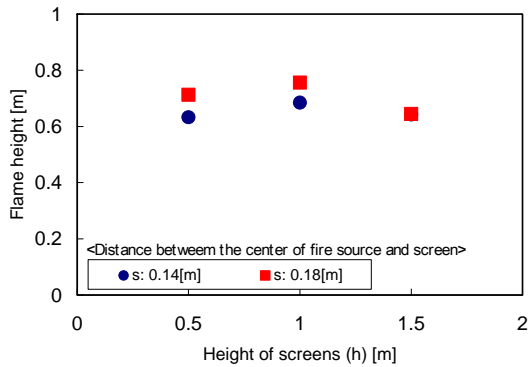


Figure 7. Height of whirling flames in case of changing height of the screens ($Q:15[\text{kW}]$, $c:0.05[\text{m}]$, $s:0.14, 0.18[\text{m}]$)



Figure 8. Comparison of observed flame of free burning and whirling flame

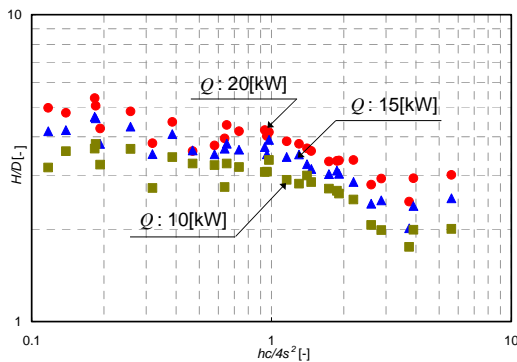


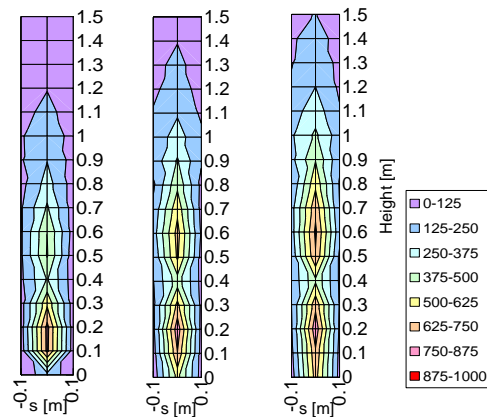
Figure 9. Height of observed whirling flame

As the experimental result, the height of observed whirling flame for taking $hc/4s^2$ in the x axis and H/D in the y

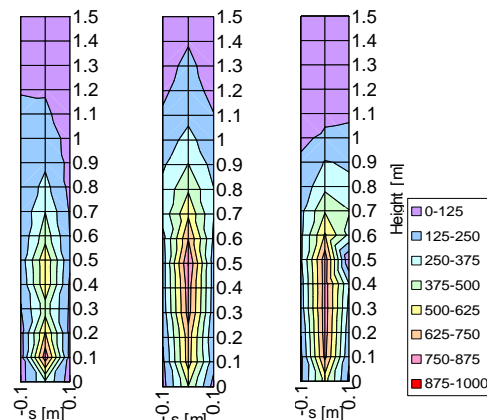
axis was shown in Figure 9. H/D decreases as $hc/4s^2$ increases. The above tendency is common to all the experimental patterns. Moreover, the height of the whirling flame depends on the heat release rate.

(2) Temperature of whirling flames

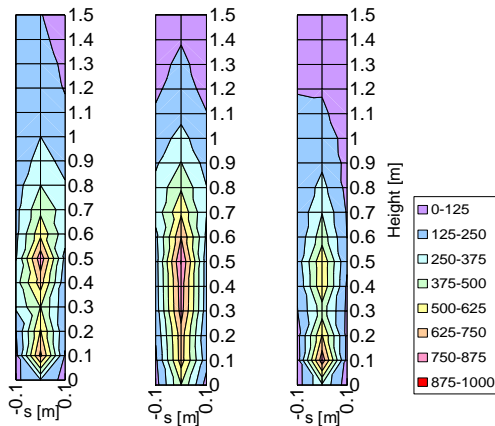
The distribution of vertical temperature was measured for two minutes every two seconds, and the average of the measured value was shown in Figure 10 and 11 as example. As a general tendency, the constriction in the flame core was generated by the effect on the whiling motion in a certain height.



($Q:10[\text{kW}]$) ($Q:15[\text{kW}]$) ($Q:20[\text{kW}]$)
a) $h:1.5[\text{m}]$, $s:0.24[\text{m}]$, $c:0.05[\text{m}]$



($h:1.5[\text{m}]$) ($h:1.0[\text{m}]$) ($h:0.5[\text{m}]$)
b) $Q:20[\text{kW}]$, $s:0.18[\text{m}]$, $c:0.05[\text{m}]$



($c:0.05[m]$) ($c:0.10[m]$) ($c:0.15[m]$)
 c) $Q:20[kW]$, $s:0.16[m]$, $h:1.5[m]$

Figure 10. The distribution of vertical temperature

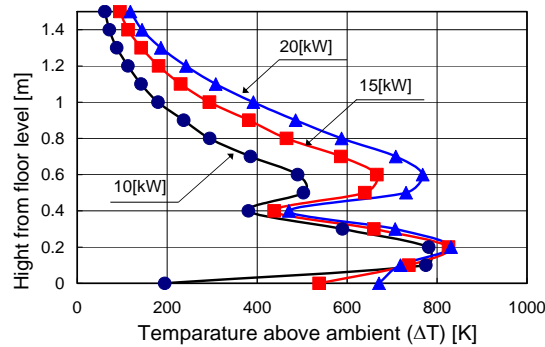


Figure 11. Vertical temperature distribution of trajectory of flame

(3) Horizontal flow velocity of flame

The measurement results of the horizontal flow velocity distribution at 0.3 [m] using by the PIV system are shown in Figure 12. The whirling motion can be confirmed. The density of flow velocity distribution in the vicinity of the center has thickened as the distance between the center of fire source and a screen expands in case other conditions are the same. That is meant that the power of the whirling motion strengthens. This tendency can be confirmed from Figure 13, too.

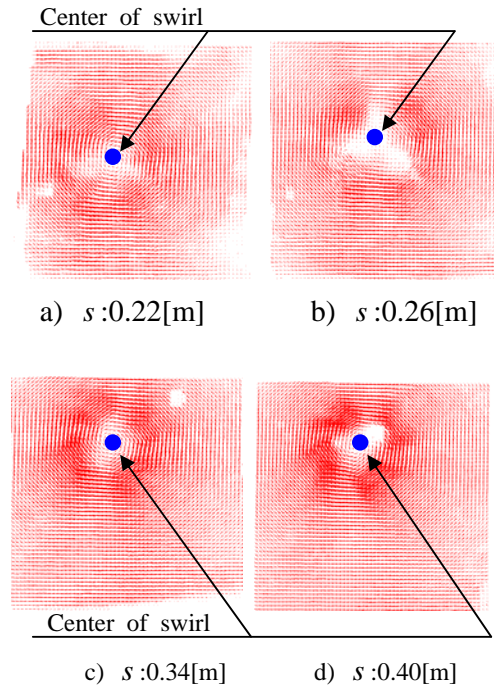


Figure 12. Flow horizontal velocity of flame at 0.3[m] height from floor level ($Q:20[kW]$, $h:1.5[m]$, $c:0.05[m]$)

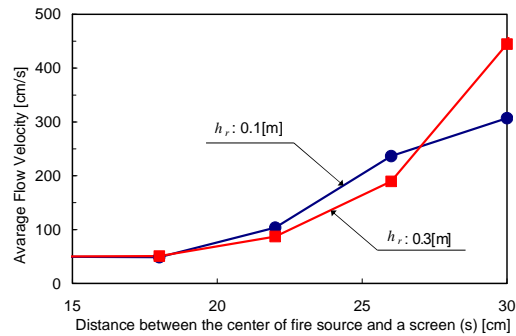


Figure 13. Flow horizontal average velocity of flame ($Q:20[kW]$, $h:1.5[m]$, $c:0.05[m]$)

3. Numerical Simulations

The effectivity of the Computational Fluid Dynamics (CFD) field model as a tool that clarified the physical mechanism of whirling flames was examined. In this study, Fire Dynamics Simulator (FDS) developed by McGrattan et al. in National

Institute of Standards and Technology (NIST) was used as a simulation code [7]. Outline of the CFD models (turbulence, combustion, radiation, etc.) used in FDS [8] were shown in the following.

3.1 Outline of FDS code

The governing equations used in FDS consist of the conservation equations of mass, momentum, energy, chemical species, and a state equation.

$$\frac{\partial \rho}{\partial t} + \nabla \cdot \rho \mathbf{u} = 0 \quad (2)$$

$$\rho \left(\frac{\partial \mathbf{u}}{\partial t} + (\mathbf{u} \cdot \nabla) \mathbf{u} \right) + \nabla p = (\rho - \rho_\infty) \mathbf{g} + \mathbf{f} + \nabla \cdot \boldsymbol{\tau} \quad (3)$$

$$\frac{\partial}{\partial t} (\rho h) + \nabla \cdot \rho h \mathbf{u} = \frac{Dp}{Dt} - \nabla \cdot \mathbf{q}_r + \nabla \cdot k \nabla T + \sum_i \nabla \cdot h_i \rho D_i \nabla Y_i \quad (4)$$

$$\frac{\partial \rho Y_i}{\partial t} + \nabla \cdot \rho Y_i \mathbf{u} = \nabla \cdot \rho D_i \nabla Y_i + m_i \quad (5)$$

$$p_0 = \rho TR \sum (Y_i / M_i) \quad (6)$$

The viscous stress tensor in the motion equation is given by the following equation.

$$\boldsymbol{\tau} = \mu \left(2 \text{def} \mathbf{u} - \frac{2}{3} (\nabla \cdot \mathbf{u}) \mathbf{I} \right) \quad (7)$$

Where, \mathbf{I} is a unit matrix. Moreover, Large Eddy Simulation (LES) using a standard Smagorinsky model as a Sub Grid Scale model (SGS) [9] is performed in FDS. Thermal and chemical species diffusion improves by mixed effect of small eddies in turbulence flow field. In an LES, thermal conductivity and chemical species diffusivity are related to the turbulent viscosity by

$$k_{LES} = \frac{\mu_{LES} C_p}{P_r} \quad (8)$$

$$(\rho D)_{i,LES} = \frac{\mu_{LES}}{Sc} \quad (9)$$

Where, P_r is the Prandtl number and Sc is the Schmidt number. In this numerical simulation, the Prandtl number P_r and the Schmidt number Sc were assumed as constant value 0.5.

3.2 Conditions of Simulation

As shown in Figure 14, the region enclosed with screens is a calculation domain. The simulation time was assumed to be 20 seconds. As for the x and the y axially, the equal intervals lattice was used. The width of one lattice cell is $2/3 \times 10^{-2}$ [m]. In this case, one side of the fire source is divided into 30 at equal intervals. As for the z axially (height), it was assumed that it divided into 80 at equal intervals. The height of one lattice cell is 1.625×10^{-2} [m]. In the top opening and the space of the screen, the condition of atmospheric open (pressure constant) was set. The outside temperature was assumed to be 20 [°C].

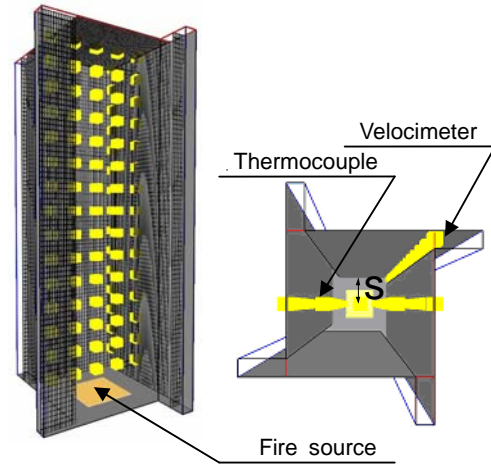


Figure 14. Schematic of the calculation domain.

3.3 Comparison between results of simulations by FDS and experiments

(1) Height of whirling flames

In Figure 15, the height of whirling flames obtained by FDS simulations and the experiment were shown in case that heat release rate (Q) was 20 [kW]. The average flame height, as shown following equation (10), in case of free burning that proposed by Heskestad [10] was shown by the solid line in Figure 15.

$$\frac{H}{D} = 3.7Q^{*2/5} - 1.02 \quad (10)$$

Where, H is the flame height [m], D is the characteristic of fuel size [m], and Q^* is the non-dimensional heat release rate [-]. The height of whirling flames obtained by the experiment doubles compared with the results of the calculation by equation (10). On the other hand, the height of whirling flames simulated by FDS code was about a half compared with the results of calculation by equation (10).

In the experiment, the tendency that the height of whirling flames expands was observed as s extended. While, in the simulation by FDS code, the tendency to which the height of whirling flames shrank was observed as s extended. It is thought that the tendency is different because burning behavior in the vicinity of the fire source surface of both is greatly different.

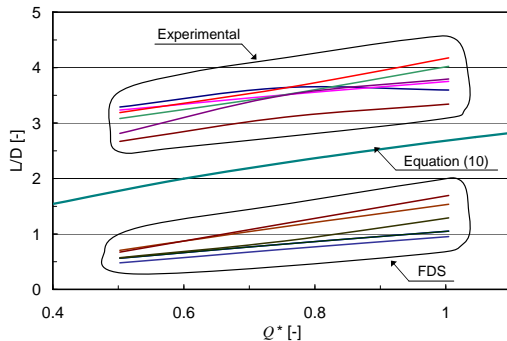
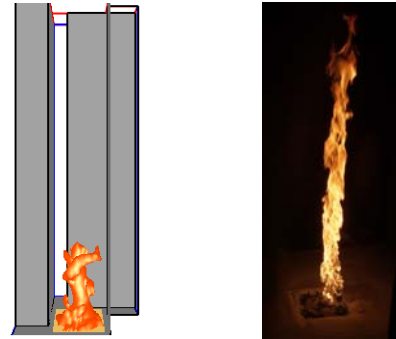


Figure 15. Average height of the flame.

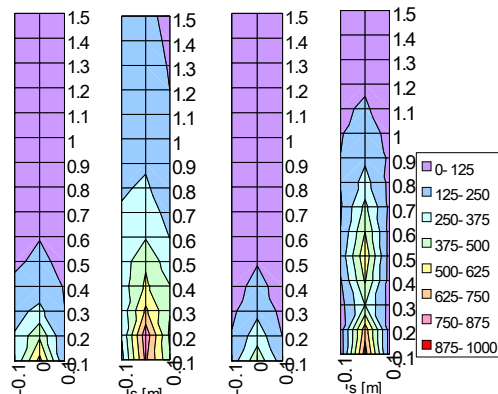


a) FDS code b) Experiment

Figure 16. Schematic average height of the flame.

(2) Temperature of whirling flames

As an example, in Figure 17, the vertical temperature distributions of flames obtained by FDS simulations and the experiments were shown in case that heat release rate (Q) was 15 [kW]. As well as the above result on the height of whirling flames, on the vertical temperature distribution of flames, the simulation results by using FDS code were lower than the experimental results. In the experiment, the radiation from the fire source influences the thermocouples. Therefore, it is necessary to consider radiation from the fire source in FDS simulations in order to obtain the results corresponding to the experiment.



a) $s : 0.1[m]$ b) $s : 0.2[m]$

Figure 17. Average temperature of the flame. (FDS, Exp.)

(3) Flow velocity of whirling flames

The results of FDS simulation and the experimental results were compared for horizontal average flow velocity of whirling flames in internal and surrounding. As an example, the comparison, Q was 20[kW], s was 0.14[m] and h_r was 0.3 [m], was shown in Figure 18. In this case, the average scalar quantity at horizontal flow velocity was 1.4452[m/s] (FDS), and 0.4465[m/s] (experiment). The horizontal average flow velocity of FDS simulation was faster than that of the experiment. A comparison of experimental results and the FDS simulation results was shown in Figure 19 in case that Q was 20 [kW]. As for the experimental results, the tendency to fast with an increase in s was observed while FDS simulation results were almost constant.

3.4 Discussions

In the above, the results FDS simulation and the experiment were compared on temperature, height, horizontal flow velocity of whirling flames. However, there were differences in the results of both because of the influence of the radiation to the thermocouple, the difference of the flame behavior in the vicinity of the fire source surface and the influences of the eddy viscosity of the eddy flow, etc. Therefore, it seems that it is necessary to improve the computing environment and the sub-model of FDS code to solve these problems. The concrete example is shown in the following.

- 1) To improve the influence of the eddy viscosity by Eddy flow, the Smagorin-ske constant should be changed.
- 2) To bring the burning behavior in the vicinity of the fire source surface, the characteristic of fuel size should be reduced.

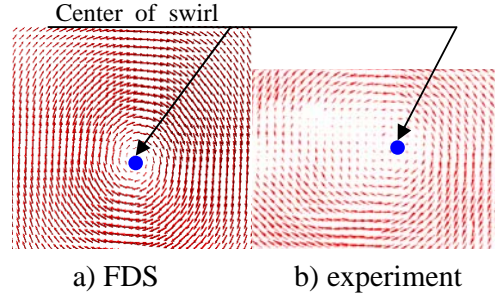


Figure 18. Comparison of average horizontal flow velocity of whirling flames (Q :20[kW] , s :0.14 [m], h :1.5[m] , c :0.05[m] , h_r :0.3[m])

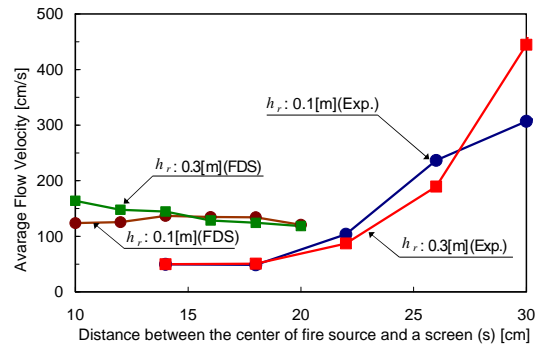


Figure 19. Average flow horizontal velocity of whirling flames (Q :20[kW] , h :1.5[m] , c :0.05[m] , h_r :0.3[m])

5. Conclusion

A systematic experiment was carried out by using the reductive scale model in order to solve the generation mechanism and properties of the fire whirls qualitatively and quantitatively in this study. As a result, it was confirmed in the following.

- The tendency that the height of whirling flames decreases as $hc/4s^2$ increases was shown.
- As for the temperature of whirling flame, the constriction (position in which the temperature lowers) is caused in certain height by the swirl.

- The average horizontal flow velocity of whirling flames shows the tendency to increase as the distance between the center of fire source and a screen (s) extends.

In addition, the results of simulation by using FDS code and the experiment were compared for the height, temperature, and flow horizontal velocity. However, the enormous discrepancy was caused in both. As a cause, it is thought that there were the following problems for FDS code.

- It is thought that the tendency is different because burning behavior in the vicinity of the fire source surface of both is greatly different.
- It is necessary to improve the influence of the eddy viscosity by Eddy flow.
- It is necessary to consider radiation from the fire source in FDS simulations in order to obtain the results corresponding to the experiment.

References

1. S. Sohma, "Tornado caused by conflagration", Journal of Japan Association for Fire Science and Engineering, Vol.24, No.2, pp.119-129, 1974 (in Japanese)
2. Central Weather station, "Investigation report of Great Kanto Earthquake", pp.1-161, 1926 (in Japanese)
3. Y. Hasemi : Modeling of the flame-cored fire Whirl, Journal of Architecture and Planning, Architectural Institute of Japan, No. 352, pp.119-124, 1985 (in Japanese)
4. K. Satoh and K. T. Yang: "Simulations of Swirling Fires Controlled by Channeled Self-generated Entrainment Flows" , Proceedings of the 5th Inter-

- national Symposium on Fire Safety Science, pp.201-212, 1997
5. H.W.Emmons and S.J.Ying: The fire whirl, Proceedings of the 11th Combustion Symposium (International), pp. 475-488, 1967
6. Y. Hayashi, T. Saga, Experimental Study on Temperature Distributions in Fire-Induced Flows, Journal of Environmental Engineering, Architectural Institute of Japan, No. 566, pp.25-32, 2003 (in Japanese)
7. URL <http://fire.nist.gov/fds/>
8. McGrattan, K. et al., Fire Dynamics Simulator (Version3)- Technical Reference Guide, NISTIR6783, 2002
9. J. Smagorinsky., Circulation Experiments with the Primitive Equations, I. The Basic Experiment. Monthly Weather Review, 1963
10. Heskestad. G., Luminous Height of Turblent Diffusion Flames, Fire Safety Journal, Vol. 5, pp.103-108, 1983

Nomenclature

- C_p : specific heat [J/kgK]
 C_s : Smagorinsky constant [-]
 c : width of the clearance between screens [m]
 D : characteristic of fuel size [m]
diffusion coefficient [m^2/s]
 g : acceleration of gravity [m/s^2]
 H : height of flame [m]
 h : height of screen [m],
enthalpy [J/kg]
 h_r : height of measurement point [m]
 k : thermal conductivity [W/mK]
 I : radiation intensity [W/m²str]
 M : molecular weight [-]
 m_l : production rate of l^{th} species per unit volume [kg/m^3s]
 P : pressure [Pa]
 P_r : Prandtl number [-]

Q : heat release rate [kW]
 Q^* : non-dimensional heat release rate [-]
 R : universal gas constant [J/kgK]
 S_c : Schmidt number [-]
 s : distance between the center of fire
source and a screen [m]
 t : time [s]
 T : temperature [K]
 Y : mass fraction [-]
 \mathbf{f} : external force vector [N/m³]
 \mathbf{q}_r : radiative heat flux vector [W/m²]
 \mathbf{u} : velocity vector [m/s]
 κ : absorption coefficient [-]
 ρ : density [kg/m density (kg/m³)]
 μ : viscosity coefficient [kg/ms]

Subscript

f : full scale
 s : reductive scale